Internal Methyl Rotation in the CH Stretching Overtone Spectra of *ortho*-, *meta*-, and *para*-Xylene

Zimei Rong and Henrik G. Kjaergaard*,†

Department of Chemistry, University of Otago, P.O. Box 56, Dunedin, New Zealand

Received: October 16, 2001; In Final Form: March 28, 2002

The room-temperature vapor phase overtone spectra of *o*-, *m*-, and *p*-xylene have been recorded in the CH stretching region corresponding to $\Delta v_{CH} = 2-6$ with conventional near-infrared spectroscopy ($\Delta v_{CH} = 2$ and 3), intracavity titanium:sapphire ($\Delta v_{CH} = 4$ and 5) and dye laser photoacoustic spectroscopy ($\Delta v_{CH} = 6$). Absolute oscillator strengths have been measured from the conventional spectra and relative oscillator strengths within a given overtone from the conventional and photoacoustic spectra. The aryl region of the spectra can be interpreted simply in terms of a number of nonequivalent and independent local modes. The methyl region of the spectra is more complex. The methyl band profiles in the overtone spectra of *m*-xylene and *p*-xylene are very similar to each other and to that of toluene and differ significantly from the methyl band profiles in the spectra of *o*-xylene. We use a simple anharmonic oscillator local mode model with ab initio calculated dipole moment functions to calculate oscillator strengths of the aryl transitions. The methyl band profiles are simulated on the basis of a model that incorporates the harmonically coupled anharmonic oscillator local mode model for the CH stretching modes and a rigid rotor basis for the methyl internal rotation (torsion). The model parameters are calculated ab initio. The dipole moment function is expressed in a series expansion in both the CH displacement coordinate and the torsional angle whereas the frequency, anharmonicity, and torsional potential are expressed in Fourier series of the torsional angle. The difference in the methyl band profiles in *o*-xylene, and in *m*- and *p*-xylene are ascribed mainly to differences in the torsional potential and the dipole moment function. Our simulations have successfully reproduced the methyl band profiles in the xylene spectra and the relative aryl to methyl intensities.

Introduction

In our previous paper on the overtone spectra of toluene-d_0, -α-d_1 and -α-d_2,[1] we successfully reproduced the observed methyl band profiles in the higher CH stretching overtone regions. Our model accounted well for changes in methyl band profiles between the three molecules with different degrees of deuteration of the methyl group. We illustrated the importance of coupling between CH stretching and methyl torsion motion and showed that the coupling between the three CH stretching oscillators is less important than the coupling between the CH stretching and methyl torsion for the higher overtone ($\Delta v_{CH} > 2$). The methyl group was described by a harmonically coupled anharmonic oscillator (HCAO) local mode model[2−7] for the CH stretching vibrations and in a rigid rotor basis for the methyl torsion. We used an adiabatic approximation to separate the CH stretching vibrations from the methyl torsion. The barrier to internal rotation in toluene is small and has 6-fold (V_6) symmetry. The variation in the CH stretching frequency and anharmonicity with torsional angle (θ) was described by a constant plus cos(2θ) term thereby providing an additional barrier to the methyl internal rotation. Kjaergaard et al. had earlier shown that the dipole moment function was well approximated by a limited Fourier series in the torsional angle (constant plus first non zero angular dependent term).[8,9] Within this approximation, the total intensity for the methyl CH stretching group can be found by averaging over the methyl internal rotation.[8] In the previous papers, we used this simple approach to predict relative aryl to methyl CH stretching overtone intensities.[8,9] These relative intensities were in good agreement with the methyl to aryl relative intensities obtained in the later paper,[1] where we simulated the methyl band profile and not simply averaged over the torsional angle.

The xylene series of molecules have added complexity. Previously, Gough and Henry measured the CH stretching overtone spectra of *o*-, *m*-, and *p*-xylene heated to 86 °C with long path length conventional spectroscopy in the $\Delta v_{CH} = 3$ and 4 regions.[10] They found an apparent three peak structure in the methyl $\Delta v_{CH} = 3$ and 4 regions of the *m*- and *p*-xylene similar to what is observed in the spectra of toluene.[1−3,10] The spectra of *o*-xylene in the methyl $\Delta v_{CH} = 3$ and 4 regions are quite different with only two distinct peaks.[10] The experimental barrier to internal rotation in *m*- and *p*-xylene is found to have 6-fold symmetry with a barrier height of 25 and 10 cm^{-1}, respectively, which is similar to the 5 cm^{-1} barrier in toluene and one might expect similar methyl region spectra.[11,12] In molecules such as propane and dimethyl ether, the barrier to methyl torsion has 3-fold symmetry (V_3) with a relatively high torsional barrier. Thus, the methyl group is relatively fixed in a single preferred conformation relative to the frame and has two nonequivalent methyl CH bonds, the out-of-plane and the in-plane.[13,14] The difference in bond length, which leads to differences in the CH stretching frequencies is reflected in two distinct peaks in the overtone spectra of propane and dimethyl ether.[13,14] The experimental barrier to methyl internal rotation

* To whom correspondence should be addressed. E-mail: henrik@alkali.otago.ac.nz. Fax: 64-3-479-7906. Phone: 64-3-479-5378.

† On sabbatical at Cooperative Institute for Research in Environmental Sciences (CIRES), University of Colorado, Boulder Colorado 80309-0216.

10.1021/jp013838x CCC: $22.00
Published on Web 06/07/2002

in *o*-xylene has 3-fold symmetry with a V_3 barrier of 425 cm^{-1} and a smaller V_6 barrier of 18 cm^{-1}.[12] Thus the two peak structure observed in the *o*-xylene methyl region spectra is perhaps not surprising. Previously, Anastakos and Wildman[15] attempted to simulate the $\Delta\upsilon_{CH} = 3$ and 4 methyl regions of the toluene and *o*-xylene spectra with a model that describes the CH stretching in a harmonic oscillator basis and the methyl torsion in a rigid rotor basis. They used a linear approximation of the dipole moment function and assumed this dipole moment function to be independent of the torsional angle. We have shown that a linear dipole moment function is insufficient for the calculation of overtone transitions intensities.[13,14,16]

Cavagnat et al. have successfully simulated the methyl profiles in the spectra of nitromethanes,[17−19] toluenes[20,21] and methylpyridine-4-α-d_2,[22] all molecules with small 6-fold torsional barriers. In the molecules with CH_3 groups they considered the effect of Fermi resonance between CH stretching and HCH bending vibrations. Cavagnat et al. included rotation of the whole molecule as the convolution profile for each of the transition. This seemed to improve the agreement in the fundamental and first overtone regions. They used an ab initio calculated dipole moment function expanded in both the CH stretching displacement coordinates and torsional angle.[17−23] Recently, Cavagnat et al. also simulated methyl band profiles in the $\Delta\upsilon_{CH} = 1-4$ spectra of methylpyridine-2-α-d_2 and methylpyridine-3-α-d_2. These molecules have 3-fold torsional barrier heights of 90 and 50 cm^{-1}, respectively. Due to the deuteration the CH stretching problem is limited to a single CH bond.[23] They successfully reconstructed their experimental spectra for these two molecules.

Zhu et al. developed a model to simulate the methyl band profiles of the $\Delta\upsilon_{CH} = 2-6$ regions in the overtone spectra of 2,6-difluorotoluene, a molecule with a small (approximately 46 cm^{-1}) V_6 torsional barrier.[24] Their model included the HCAO local mode model to treat the three CH bonds of the methyl group and a rigid rotor basis for the methyl torsion. The methyl spectra were successfully predicted and attributed to a large number of transitions that arise from terms involving torsion-stretch coupling both in the Hamiltonian and in the dipole moment function.[24]

In this paper, we generalize the previous model for the CH_3 group[1,24] to allow arbitrary symmetry and magnitude of the torsional potential. We approximate the potential energy, frequency, and anharmonicity by a sixth order Fourier series in the torsional angle and include coupling between the CH stretching oscillators and between CH stretching and torsion. The dipole moment function is approximated by a Fourier series in the torsional angle and a Taylor series in the CH stretching displacement coordinates.

Experimental Section

The samples *o*-xylene (Aldrich, anhydrous 97%), *m*- and *p*-xylene (Aldrich, anhydrous 99+%), were used without further purification except for degassing. The room-temperature vapor phase overtone spectra of *o*-, *m*-, and *p*-xylene were recorded in the $\Delta\upsilon_{CH} = 2$ and 3 regions with conventional absorption spectroscopy and in the $\Delta\upsilon_{CH} = 4-6$ regions with intracavity laser photoacoustic spectroscopy (ICL-PAS).

Our conventional spectrophotometer (Cary 500 Scan UV−vis−NIR) was fitted with a 4.8 m long path White cell (Infrared Analysis Inc.) with Infrasil quartz windows. Background scans with an evacuated cell were recorded and subtracted for each of the sample spectra. The experimental absolute oscillator strength f of an absorption band can be determined from these conventional spectra and the following equation[25]

$$f = 2.6935 \times 10^{-9}[\mathrm{K}^{-1}\ \mathrm{Torr\ m\ cm}]\frac{T}{pl}\int A(\tilde{\nu})d\tilde{\nu} \qquad (1)$$

where T is the temperature, p the pressure, l the path length, A the absorbance, and $\tilde{\nu}$ the frequency in cm^{-1}.

Our version of ICL-PAS is similar to other versions that have been described previously.[26,27] Briefly, a Coherent Innova Sabre argon ion laser running at all lines was used to pump either a Coherent 890 broadband titanium:sapphire laser (15 W pump power) or a Coherent 599 broadband dye laser (12 W pump power). The mid- and short-wave optics were used with the titanium:sapphire laser to measure the $\Delta\upsilon_{CH} = 4$ and 5 regions, respectively. The $\Delta\upsilon_{CH} = 6$ region was recorded with the dye laser and the dyes DCM and R6G for the methyl and aryl regions, respectively. The photoacoustic cell contained a Knowles Electronics EK3132 electret microphone. The photoacoustic signal from the microphone was amplified 30 dB (30 times), and sent to a Stanford Research Systems SR830 lock-in amplifier. The argon ion laser was intensity modulated with a Stanford Research Systems SR540 mechanical chopper, and the lock-in amplifier was referenced to the modulation frequency. The titanium:sapphire or dye laser output power was measured with a Coherent LaserMate-Q power meter fitted with a 1000:1 attenuator. The power meter output was sent to an Agilent 34401A digital multimeter after voltage integration with a resistor-capacitor (RC) circuit and was used to normalize the photoacoustic signal. Corrections were made for both the silicon detector response curve and the output coupler transmission curve. The titanium:sapphire and dye lasers were tuned with a three plate birefringent filter rotated by a stepper motor. The three plate birefringent filter gives a resolution of about 1 cm^{-1}. Our photoacoustic apparatus is computer controlled through a National Instruments IEEE interface. The wavelength calibration of the scans was conducted with a Burleigh WA-1000 wavemeter. The photoacoustic cell was filled with argon buffer gas at pressures of about 200 Torr to increase the photoacoustic signal.[28,29] The absolute absorbance of a sample is not known with our ICL-PAS apparatus, however relative intensities can be obtained in the ICL-PAS spectra.

Galactic Grams/32 (v5.03) software was utilized for spectral curve fitting of the overtone spectra. Spectral bands were curve-fitted with Lorentzian line shapes and a linear baseline with no other constraints applied to the curve-fitting procedure.

Theory and Calculations

The oscillator strength f_{eg} of a vibrational transition from the ground state g to a vibrationally excited state e is given by[13,25]

$$f_{eg} = 4.702 \times 10^{-7}[\mathrm{cm\ D}^{-2}]\tilde{\nu}_{eg}|\vec{\mu}_{eg}|^2 \qquad (2)$$

where $\tilde{\nu}_{eg}$ is the vibrational transition frequency in cm^{-1} and $\vec{\mu}_{eg} = \langle e|\vec{\mu}|g\rangle$ is the transition dipole moment matrix element in debye (D). We have used an anharmonic oscillator isolated CH local mode model to obtain the vibrational wave functions and energies of the aryl CH stretching oscillators. The vibrational wave functions and energies of the methyl group are obtained with the CH stretching oscillators described by the HCAO local mode model and the internal rotation of the methyl group in a rigid rotor basis. The dipole moment functions for both aryl and methyl bonds are obtained from a series of ab initio calculations. The dipole moment functions are expanded in the internal CH displacement coordinates q_i and for the methyl group also the torsional angle θ.

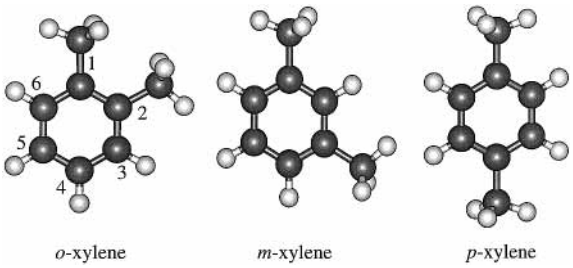

Figure 1. Schematic diagram of the HF/6-31G(d) optimized geometries of *o*-xylene (left), *m*-xylene (middle) and *p*-xylene (right) and the numbering of the carbon atoms on the ring. The aryl CH bond lengths are as follows: in *o*-xylene $R_3 = R_6 = 1.0763$ Å and $R_4 = R_5 = 1.0756$ Å, in *m*-xylene $R_2 = 1.0775$ Å, $R_4 = 1.0767$ Å, $R_5 = 1.0759$ Å and $R_6 = 1.0761$ Å and in *p*-xylene $R_2 = R_3 = 1.0771$ Å and $R_5 = R_6 = 1.07645$ Å.

Aryl CH Oscillators. The coupling between CH bonds attached to different C atoms is very small.[30] Thus, the aryl CH bonds can, to a very good approximation, be described by isolated Morse oscillators, one for each of the nonequivalent aryl CH bonds. Briefly, the Hamiltonian for an isolated CH stretching Morse oscillator can be written[8]

$$H/hc = \left(v_j + \frac{1}{2}\right)\tilde{\omega}_j - \left(v_j + \frac{1}{2}\right)^2 \tilde{\omega}_j x_j \qquad (3)$$

where $\tilde{\omega}_j$ and $\tilde{\omega}_j x_j$ are the local mode frequency and anharmonicity (in cm^{-1}) of the CH_j oscillator. The eigenstates of the Hamiltonian are denoted by $|v_j>_j$, where v_j is the vibrational quantum number and the eigenstates are Morse oscillator wave functions. The local mode parameters, $\tilde{\omega}$ and $\tilde{\omega}x$, for the aryl CH oscillators were derived from the observed local mode peak positions. The low barriers to internal rotation of the methyl groups in particular in *m*- and *p*-xylene give rise to a number of possible conformers. Thus one might expect a number of aryl CH stretching overtone transitions. However, the aryl CH bonds change very little upon rotation of the methyl groups, and based on the calculated CH bond lengths for various methyl rotations, we would expect one peak in the aryl region of the overtone spectra of the *p*-xylene, three peaks for *m*-xylene and two peaks for *o*-xylene, in agreement with the observed spectra. The ab initio optimized structures of the xylene molecules are given in Figure 1.

We expand the dipole moment function for each of the aryl CH bonds in the internal displacement coordinate q_i as described in previous papers.[8,30] We limit the expansion to sixth order in the coordinate q_i. The expansion coefficients are found from a grid along q_i of ab initio calculated dipole moments. We use a 15 point grid from −0.3 Å to 0.4 Å displacements with a step size of 0.05 Å. The 15 point grids are fitted to a sixth order polynomial with use of a polyfit function of MATLAB.[31] The optimized structures and all grid points were calculated at the Hartree−Fock self-consistent field level of theory and the 6-31G(d) basis set with use of GAUSSIAN94.[32] We have previously used a 9 point grid in the range from −0.2 Å to 0.2 Å with a step size of 0.05 Å to determine the expansion coefficients. The larger grid used in the present work ensure better convergence of the higher order expansion coefficients which is mainly important to obtain reasonable accuracy in the angular dependence of the dipole moment expansion coefficients for the methyl rotor [vide infra].

Methyl Coordinate System. The coordinate system used to define the internal rotation of the methyl group is shown in Figure 2. The Hamiltonian and the dipole moment function of the methyl group including both the CH stretching and torsion

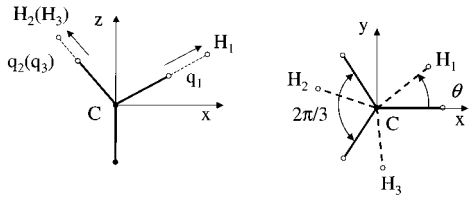

Figure 2. Coordinate system used to describe the rotating methyl group. The projection of the methyl group on the *xz* plane is shown to the left with illustration of the CH stretching displacement coordinates, q_i. The figure to the right shows the projection on the *xy* plane. The methyl group illustrated by the dashed lines has been rotated θ degrees from the minimum energy conformer shown with solid lines. The torsional angle $\theta_1 = \theta$, $\theta_2 = \theta + 2\pi/3$ and $\theta_3 = \theta - 2\pi/3$. The ring is in the *xz* plane.

are described within this coordinate system. The coordinate system is fixed to the molecular frame of the ring. The positive *z*-direction is from the carbon atom on the ring (C) toward methyl carbon atom and the carbon ring is in the *xz* plane. The positive *x*-axis direction is toward the first hydrogen atom (H_1). The positive *y*-axis is defined by a right-hand rule. The hydrogen atom at positive *y* is numbered as the second hydrogen atom (H_2). The projections of the methyl group on the *xz* and *xy* planes are illustrated in the left and right side of Figure 2, respectively. The torsional angle of the methyl group, $\theta = \theta_1$, is defined as the dihedral angle between the plane consisting of the first CH_1 bond and *z*-axis and the *xz* plane. The positive torsional angle is defined from the positive *x*-axis counterclockwise toward the positive *y*-axis. We also define torsional angles to the other two CH bonds in a rigid approximation as $\theta_2 = \theta_1 + 2\pi/3$ and $\theta_3 = \theta_1 - 2\pi/3$.

Methyl Hamiltonian. The variation with torsional angle of the calculated potential energy (*V*), CH stretching frequency (Ω), and anharmonicity (*X*) of *p*-xylene and *o*-xylene is shown in Figure 3. The variation for *p*-xylene is very similar to that of toluene as expected. However, the functional forms of the potential, frequency and anharmonicity for *o*-xylene are no longer as simple. We fit the functional forms of the potential, frequency and anharmonicity to a Fourier series limited to the sixth order. This leads to a total of 13 terms, which we express as a column vector $F_i = [1, \cos(\theta_i), \cdots \cos(6\theta_i), \sin(\theta_i), \cdots \sin(6\theta_i)]^T$ with a dimension of 13. We will show this to be a good approximation.

We approximate the total Hamiltonian for a rotating methyl group by

$$\begin{aligned} H_{v_1 v_2 v_3 m}/hc &= H_v + H_t + H_{v-v} + H_{v-t} \\ &= \sum_{i=1}^{3}\left[\Omega F_i\left(v_i + \frac{1}{2}\right) - XF_i\left(v_i + \frac{1}{2}\right)^2\right] + VF_1 + Bm^2 \\ &\quad - \gamma'(a_1 a_2^{+} + a_1^{+} a_2 + a_2 a_3^{+} + a_2^{+} a_3 + a_3 a_1^{+} + a_3^{+} a_1) \end{aligned} \qquad (4)$$

where Ω and *X* are the Fourier series expansion coefficients for the frequency and anharmonicity expressed as row vectors with a dimension of 13. The indices refer to the three CH_i bonds and torsional angles θ_i defined in Figure 2. The methyl torsional Hamiltonian (H_t) is $VF_1 + Bm^2$, where VF_1 is the torsional potential and *B* is the rotational constant. We ignore the small variation in *B* with torsional angle and vibrational excitation. The γ' term in eq 4 is the intramanifold harmonic coupling between the CH stretching oscillators (H_{v-v}) and the small variation of the effective coupling coefficient γ' with θ is ignored. The a and a^+ are the well-known ladder operators.

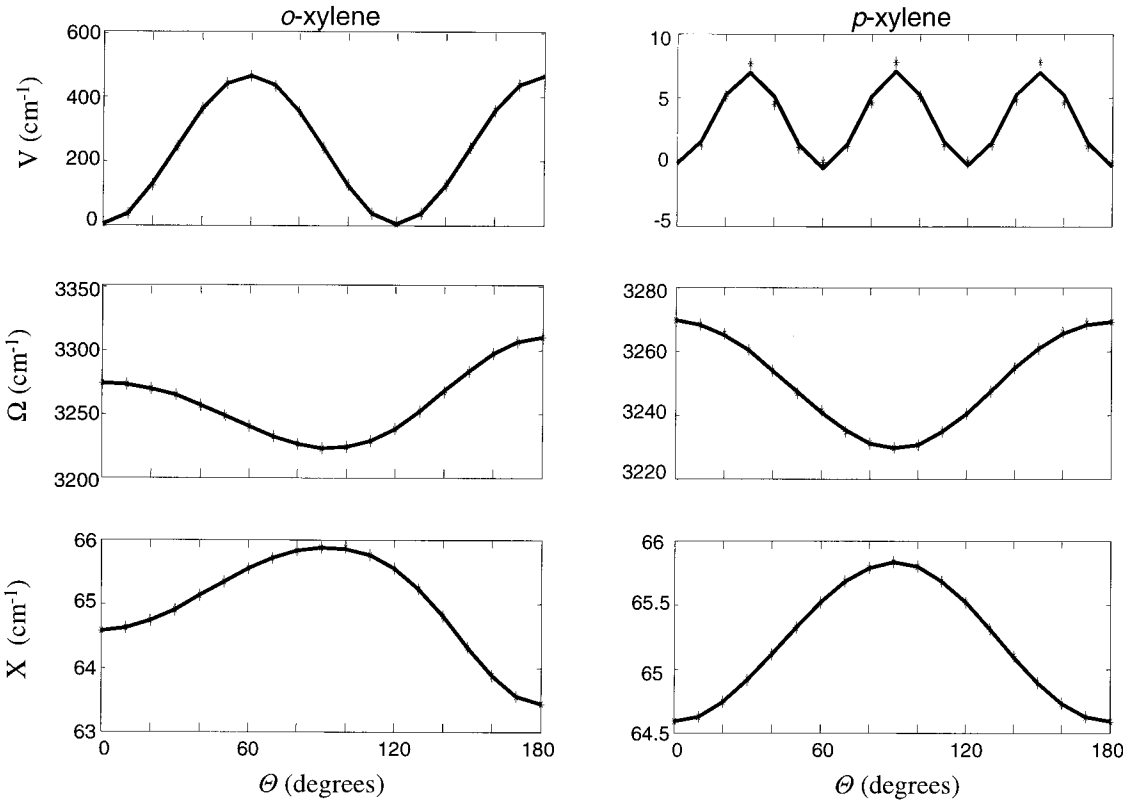

Figure 3. Potential (V), frequency (Ω) and anharmonicity (X) of *o*- and *p*-xylene as a function of the torsional angle, θ. The asterisks represent the ab initio calculated results and the solid lines the Fourier series fit.

The summation contains both the CH stretching part of the Hamiltonian (H_v) and the CH stretching torsional coupling part (H_{v-t}). H_v is obtained from the first term in the F_i vectors. In our model, the three CH oscillators are equivalent except for the phase which is included in F_i. The Hamiltonian in our previous paper can be expressed by eq 4 if only the 1 and the $\cos(2\theta_i)$ terms in the F_i are retained.

We assume that the two methyl groups in *o*-, *m*-, and *p*-xylene are equivalent and include only one methyl group in our model explicitly. The other methyl group is part of the frame. The effect of the frame is seen in the potentials, frequencies, anharmonicities and dipole moment functions, which are different for the three xylenes.

The coefficient vectors Ω, X, and V are obtained from a series of ab initio calculations in a two-step process. The CH stretching frequency and anharmonicity can be determined from the second and third-order derivatives of the potential energy with respect to the CH stretching displacement coordinate.[33,34] We have shown that a 9 point grid (potential energy curves) displaced from -0.2 Å to 0.2 Å with a step size of 0.05 Å is sufficient to obtain converged second and third-order derivatives of the potential energy.[33] We calculate a 9 point grid for the CH_1 oscillator to obtain the potential energy, frequency and anharmonicity. We repeated this process for each 10 degrees rotation of the methyl group from 0° to 180°. Initially, at each new torsional angle, the molecular geometry is fully optimized with a fixed torsional angle before the CH_1 stretching grid is calculated. The calculated frequencies, anharmonicities and potential energies (all in cm^{-1}) of *o*- and *p*-xylene as a function of the torsional angle are shown as the asterisks in Figure 3. We have used a MATLAB[31] program to fit the calculated frequencies, anharmonicities and potential energies at various torsional angles to a Fourier series in the torsional angle θ_1. The Fourier expansion coefficients obtained from this fitting procedure are given in Table 1 and the fitted Fourier functions are shown in Figure 3.

The vibrational torsional basis functions are a product of three Morse oscillator wave functions $|v_1>|v_2>|v_3>$ multiplied with a real rigid rotor function $|m>$. The real rigid rotor basis functions are essentially $\cos(m\theta)$ and $\sin(m\theta)$ functions, where m the torsional quantum number. We have limited m to 12, thus including a total of 25 torsional states associated with each vibrational basis function. Coupling in the model is limited to states with the same $v = v_1 + v_2 + v_3$ and the total number of vibrational-torsion states for a given v is $(2m + 1)(v + 1)(v + 2)/2$. The eigen energies and associated eigenfunctions are obtained from a diagonalization of the Hamiltonian in eq 4 in the $|v_1>|v_2>|v_3>|m>$ basis.

Methyl Dipole Moment Function. We have approximated the dipole moment function by a series expansion in the CH stretching coordinates and the torsional angle. We write the expansion in a matrix form similar to the Hamiltonian. We have left out the permanent dipole moment as it does not contribute to the vibrational transition intensities. The x component of the dipole moment vector can then be written

$$\mu_x = \sum_{i=1}^{3} Q_i C_x F_i \qquad (5)$$

where $Q_1 = [q_1, q_1^2, q_1^3, q_1^4, q_1^5, q_1^6, q_2q_3, q_2^2q_3, q_2q_3^2]$ with the CH displacement coordinates q_1, q_2 and q_3 defined in Figure 2. The Q_2 and Q_3 vectors are obtained from Q_1 by permutation of indices in the Q_1 definition. The Fourier series column vectors F_i were defined previously. The dipole moment function expansion coefficients are contained in the 9×13 matrix C_x. The y and z components of the dipole moment vector are expressed by similar equations with the expansion coefficient matrixes, C_y and C_z, respectively. The dipole coefficient matrixes

TABLE 1: Potential, Frequency and Anharmonicity as a Function of Torsional Angle for *o*-, *m*-, and *p*-Xylene[a]

molecule	parameter	1	cos(θ)	cos(2θ)	cos(3θ)	cos(4θ)	cos(5θ)	cos(6θ)
o-xylene	expt. V^b	221.5			−212.5			−9.0
	calc. V^c	235.1	1.4	1.8	−231.4	−1.6	−1.6	−4.4
	calc. Ω^c	3058.4	−10.7	32.4	−6.1	0.6	−0.1	−0.2
	calc. X^c	59.7	0.3	−0.8	0.2	−0.1	0.0	0.0
m-xylene	expt. V^b	12.5						−12.5
	calc. V^c	3.2	0.0	0.0	0.3	0.1	0.0	−3.7
	calc. Ω^c	3054.0	−0.1	18.7	−0.1	−0.7	0.3	−0.1
	calc. X^c	59.8	0.0	−0.5	0.0	0.0	0.0	0.0
p-xylene	expt. V^b	5.0						−5.0
	calc. V^c	3.3	0.0	0.0	0.1	0.1	0.0	−3.7
	calc. Ω^c	3052.3	−0.1	18.7	0.0	−0.6	0.3	0.0
	calc. X^c	59.9	0.0	−0.6	0.0	0.0	0.0	0.0

[a] The sixth order Fourier series expansion coefficients of the potential (V), frequency (Ω), and anharmonicity (X) in cm^{-1}. [b] The experimental potentials in ref 12 have been converted from the conventional form $(V_{3n}/2)[1 - \cos(3n\theta)]$ to the Fourier series. [c] Calculated with the HF/6-31G(d) method. The calculated frequencies and anharmonicities have been scaled with the scaling factors of 0.9377 and 0.907, respectively.

TABLE 2: Ab Initio HF/6−31(d) Dipole Moment Function Expansion Coefficients of Methyl Stretching and Torsion for *o*-Xylene[a]

C_x	units	1	cos(θ)	cos(2θ)	cos(3θ)	cos(4θ)	cos(5θ)	cos(6θ)	sin(θ)
q_1	debye/Å	−0.017	−0.626	−0.029	0.009	−0.004	−0.001	0.002	
q_1^2	debye/Å^2	−0.042	−1.026	−0.025	0.041	−0.009	0.000	0.000	
q_1^3	debye/Å^3	−0.020	0.246	−0.009	0.052	−0.008	0.003	−0.001	
q_1^4	debye/Å^4	0.016	−0.166	0.007	−0.024	0.002	0.003	0.000	
q_1^5	debye/Å^5	0.020	0.195	0.016	−0.035	−0.002	0.002	0.001	
q_1^6	debye/Å^6	0.004	−0.032	−0.004	0.024	0.002	−0.001	0.002	
q_2q_3	debye/Å^2	0.013	−0.312	0.003					
$q_2q_3^2$	debye/Å^3	0.002	−0.015						0.227
$q_2^2q^3$	debye/Å^3	0.002	−0.015						−0.253
C_y		1	cos(θ)	sin(θ)	sin(2θ)	sin(3θ)	sin(4θ)	sin(5θ)	sin(6θ)
q_1	debye/Å			−0.668	0.006	0.006	0.001	0.001	0.000
q_1^2	debye/Å^2			−1.202	−0.019	0.029	−0.003	0.000	−0.001
q_1^3	debye/Å^3			0.216	−0.015	0.047	−0.009	0.003	−0.001
q_1^4	debye/Å^4			−0.160	−0.002	−0.022	−0.001	0.004	−0.001
q_1^5	debye/Å^5			0.241	0.012	−0.026	−0.002	0.004	0.000
q_1^6	debye/Å^6			0.024	0.007	0.018	0.007	−0.001	0.001
q_2q_3	debye/Å^2			−0.295	0.000				
$q_2q_3^2$	debye/Å^3	−0.001	0.216	−0.015					
$q_2^2q_3$	debye/Å^3	0.001	−0.216	−0.020					
C_z	units	1	cos(θ)	cos(2θ)	cos(3θ)	cos(4θ)	cos(5θ)	cos(6θ)	sin(θ)
q_1	debye/Å	−0.543	−0.011	0.016	−0.006	−0.009	−0.003	0.000	
q_1^2	debye/Å^2	−0.888	−0.019	0.166	0.005	−0.009	−0.006	0.001	
q_1^3	debye/Å^3	−0.047	0.020	0.127	−0.001	0.011	−0.002	0.000	
q_1^4	debye/Å^4	0.154	−0.001	0.013	−0.001	0.009	0.000	−0.002	
q_1^5	debye/Å^5	0.098	−0.015	−0.011	−0.003	0.009	0.001	0.000	
q_1^6	debye/Å^6	0.051	−0.007	−0.098	−0.001	0.000	0.002	0.003	
q_2q_3	debye/Å^2	0.397	−0.003	0.091					
$q_2q_3^2$	debye/Å^3	0.080	0.008						−0.005
$q_2^2q_3$	debye/Å^3	0.080	0.008						−0.030

[a] The dipole moment function is expanded in the CH stretching coordinate as a Taylor series and the torsional coordinate in a Fourier series. The terms that are zero by symmetry have been left out. For the x and z components, the sin($m\theta$) diagonal and second order mixed stretching terms are zero. For the y component, the cos($m\theta$) diagonal and second order mixed stretching terms are zero.

are the same for the three Q_i vectors as the three CH oscillators are equivalent except for the phase difference, which is contained in the F_i column vector. The dipole moment function expansion coefficient matrixes are determined from a series of ab initio calculations similar to the procedure used to determine the coefficient vectors V, Ω and X. First at a given torsional angle, the CH_1 bond is displaced from its equilibrium position from −0.3 Å to 0.4 Å with a step size of 0.05 Å to generate a 15 point grid. This 15 point grid is then fitted to a sixth order polynomial in the CH stretching coordinate, q_1, to obtain diagonal expansion coefficients. This process is then repeated for each 10° rotation of the methyl group from 0° to 180°. The angular dependence of the diagonal dipole expansion coefficients can now be found by fitting in turn each order of the Taylor expansion to a sixth order Fourier series with our MATLAB least-squares fitting program.[31] Part of these grids were calculated to obtain the angular dependence of the coefficient vectors Ω, X, and V. The mixed expansion terms in Q_1 require a two-dimensional grid to be calculated. The intensities are less sensitive to these coefficients, and the coefficients can be found with reasonable accuracy from a 5 × 5 grid in which two CH displacement coordinates are displaced from −0.1 to 0.1 Å with a 0.05 Å step size.[13,16] We have calculated these two-dimensional grids only at the torsional angles of 0°, 90°, and 180° and limit the Fourier series for q_2q_3 to the second order and for $q_2q_3^2$ and $q_2^2q_3$ to the first order. All grid points and the optimized geometries at each torsional angle were calculated with the HF/6-31G(d) method and Gaussian 94.[32] The dipole

TABLE 3: Ab Initio HF/6−31(d) Dipole Moment Function Expansion Coefficients of Methyl Stretching and Torsion for *m*-Xylene[a]

C_x		1	cos(θ)	cos(2θ)	cos(3θ)	cos(4θ)	cos(5θ)	cos(6θ)	sin(θ)
q_1	debye/Å	−0.014	−0.628	−0.002	−0.004	−0.001	−0.001	0.001	
q_1^2	debye/Å^2	−0.023	−1.044	0.001	0.025	−0.001	−0.003	0.002	
q_1^3	debye/Å^3	−0.001	0.219	0.004	0.038	0.000	0.001	0.001	
q_1^4	debye/Å^4	0.003	−0.149	0.001	−0.026	0.001	0.003	−0.001	
q_1^5	debye/Å^5	0.004	0.226	−0.002	−0.028	0.000	0.002	0.000	
q_1^6	debye/Å^6	0.000	−0.029	−0.001	0.022	0.000	0.000	0.000	
q_2q_3	debye/Å^2	0.009	−0.317	−0.001					
$q_2q_3^2$	debye/Å^3	0.004	−0.011						0.236
$q_2^2q_3$	debye/Å^3	0.004	−0.011						−0.235
C_y		1	cos(θ)	sin($\theta\theta$)	sin(2θ)	sin(3θ)	sin(4θ)	sin(5θ)	sin(6θ)
q_1	debye/Å			−0.680	0.001	0.001	−0.001	0.001	0.000
q_1^2	debye/Å^2			−1.230	−0.001	0.018	−0.002	−0.001	0.000
q_1^3	debye/Å^3			0.243	0.000	0.032	0.000	0.000	0.000
q_1^4	debye/Å^4			−0.163	0.000	−0.022	0.000	0.002	0.000
q_1^5	debye/Å^5			0.245	0.000	−0.022	0.000	0.003	0.000
q_1^6	debye/Å^6			0.023	0.001	0.025	0.000	0.000	0.000
q_2q_3	debye/Å^2			−0.307	0.000				
$q_2q_3^2$	debye/Å^3	−0.001	0.229	−0.017					
$q_2^2q_3$	debye/Å^3	0.001	−0.229	−0.020					
C_z		1	cos(θ)	cos(2θ)	cos(3θ)	cos(4θ)	cos(5θ)	cos(6θ)	sin(θ)
q_1	debye/Å	−0.563	−0.003	0.006	−0.002	−0.007	0.000	−0.001	
q_1^2	debye/Å^2	−0.917	−0.005	0.174	−0.002	−0.008	0.001	−0.001	
q_1^3	debye/Å^3	−0.029	0.002	0.127	0.000	0.009	0.002	−0.002	
q_1^4	debye/Å^4	0.155	0.000	0.004	0.001	0.009	0.000	−0.002	
q_1^5	debye/Å^5	0.088	−0.011	−0.015	0.000	0.006	0.000	0.001	
q_1^6	debye/Å^6	0.052	0.000	−0.107	0.000	0.001	−0.001	0.004	
q_2q_3	debye/Å^2	0.441	0.000	0.095					
$q_2q_3^2$	debye/Å^3	0.073	0.000						0.004
$q_2^2q_3$	debye/Å^3	0.073	0.000						0.002

[a] The dipole moment function is expanded in the CH stretching coordinate as a Taylor series and the torsional coordinate in a Fourier series. The terms that are zero by symmetry have been left out. For the *x* and *z* components, the sin($m\theta$) diagonal and second order mixed stretching terms are zero. For the *y* component, the cos($m\theta$) diagonal and second order mixed stretching terms are zero.

moment expansion coefficient matrixes C_x, C_y and C_z for *o*-, *m*-, and *p*-xylene are given in Tables 2−4.

Computer Program. Our simulation program was written in MATLAB, which is suitable for matrix manipulation. We have used the analytical expressions to evaluate the required integrals of the displacement coordinate and the Morse oscillator wave functions.[35] The matrix size for $v = 6$ is 700 × 700, which leads to 17,500 transitions from the 25 states with $v = 0$, that contribute to the spectrum in the $\Delta v_{CH} = 6$ region.

Results and Discussion

The HF/6-31G(d) optimized geometries of *o*-, *m*- and *p*-xylene are shown in Figure 1. In all of the calculated structures the methyl groups each have one CH bond in the ring plane. In *o*- and *p*-xylene, the two out-of-plane CH bonds of one methyl group are toward to the two out-of-plane CH bonds of the other methyl group.[10,36] In *m*-xylene the two out-of-plane CH bonds of one methyl group are toward the one in-plane CH bond of the other methyl group.[10,37] Similar optimized geometries were obtained with the HF/6-311+G(d,p) method.

The experimental and calculated torsional potential expansion coefficients of *o*-, *m*- and *p*-xylene are given in Table 1 and the potentials as functions of the torsional angle are shown in Figure 3 for *o*- and *p*-xylene. We see in Figure 3 that the sixth order Fourier series fit (solid line) is a good approximation to the calculated points (asterisk) of the torsional potential. As shown in Table 1, the calculated potentials of *o*-, *m*-, and *p*-xylene agree reasonably well with the experimental ones.

On the basis of the molecular symmetry one might have expected the potential for *m*-xylene to have a 6-fold component caused by the ring and a 3-fold component due to the other methyl group. However, both the experimental and the HF/6-31G(d) calculated potentials are 6-fold. This is caused by the coupling of the two methyl groups in *m*-xylene.[37]

The local mode frequency and anharmonicity expansion coefficients of *o*-, *m*- and *p*-xylene are listed in Table 1 and the frequencies and anharmonicities as functions of the torsional angle are shown in Figure 3 for *o*- and *p*-xylene. We see in Figure 3 that the sixth order Fourier series fit (solid line) is a good approximation to the calculated points (asterisks) of the local mode frequency and anharmonicity. The angular dependence of the frequency and anharmonicity of *p*-xylene (and *m*-xylene) are very close to a constants plus cos(2θ) term, which we had used previously to model the spectra of toluene[1] and 2,6-difluorotoluene.[24] It is seen in Table 1 that the cos(θ) and cos(3θ) are significant for the frequency and anharmonicity of *o*-xylene. All sin(mθ) terms, where *m* is an integer, in the expansions disappear due to the planar symmetry of the frame.

The expansion coefficients of the dipole moment functions of *o*-, *m*- and *p*-xylene are given in Tables 2−4. The angular dependence of the first, second, and fifth order CH_1 displacement expansion coefficients of the *z* component are shown in Figure 4 for *o*- and *p*-xylene. We see in Figure 4 that the sixth order Fourier series fit (solid line) is a good approximation to the calculated points (asterisks) of the dipole moment expansion coefficients. Due to the planar symmetry of the frame the C_x and C_z coefficients have zero sin(mθ) components for the diagonal and second order mixed terms, whereas the C_y has only sin(mθ) components. Because of the lesser importance of the mixed dipole expansion terms these are limited to fewer

TABLE 4: Ab Initio HF/6−31(d) Dipole Moment Function Expansion Coefficients of Methyl Stretching and Torsion for *p*-Xylene[a]

C_x		1	cos(θ)	cos(2θ)	cos(3θ)	cos(4θ)	cos(5θ)	cos(6θ)	sin(θ)
q_1	debye/Å	0.000	−0.633	0.000	−0.005	0.000	0.000	0.000	
q_1^2	debye/Å^2	0.000	−1.055	−0.001	0.026	0.001	−0.002	0.001	
q_1^3	debye/Å^3	0.000	0.215	0.000	0.040	0.000	0.001	0.000	
q_1^4	debye/Å^4	0.000	−0.149	0.000	−0.024	0.000	0.003	0.000	
q_1^5	debye/Å^5	0.000	0.229	0.000	−0.027	0.000	0.002	0.000	
q_1^6	debye/Å^6	0.000	−0.029	0.001	0.018	0.000	0.001	−0.001	
q_2q_3	debye/Å^2	−0.001	−0.321	−0.001					
$q_2q_3^2$	debye/Å^3	0.000	−0.013						−0.234
$q_2^2q_3$	debye/Å^3	0.000	−0.013						0.253
C_y		1	cos(θ)	sin(θ)	sin(2θ)	sin(3θ)	sin(4θ)	sin(5θ)	sin(6θ)
q_1	debye/Å			−0.694	0.000	0.003	−0.001	0.001	0.000
q_1^2	debye/Å^2			−1.248	−0.001	0.022	−0.001	−0.001	0.000
q_1^3	debye/Å^3			0.239	0.000	0.033	0.000	0.000	0.000
q_1^4	debye/Å^4			−0.162	0.000	−0.022	0.000	0.002	0.000
q_1^5	debye/Å^5			0.247	0.000	−0.022	0.000	0.003	0.000
q_1^6	debye/Å^6			0.023	0.001	0.025	0.000	0.001	0.000
q_2q_3	debye/Å^2			−0.309	0.000				
$q_2q_3^2$	debye/Å^3	0.000	0.233	0.019					
$q_2^2q_3$	debye/Å^3	0.000	−0.233	0.018					
C_z		1	cos(θ)	cos(2θ)	cos(3θ)	cos(4θ)	cos(5θ)	cos(6θ)	sin(θ)
q_1	debye/Å	−0.594	0.000	0.023	0.000	−0.007	0.000	0.000	
q_1^2	debye/Å^2	−0.967	−0.002	0.205	0.000	−0.007	0.002	0.000	
q_1^3	debye/Å^3	−0.043	−0.001	0.138	0.000	0.010	0.002	−0.001	
q_1^4	debye/Å^4	0.165	0.000	−0.001	0.000	0.009	0.000	−0.002	
q_1^5	debye/Å^5	0.089	0.000	−0.016	0.000	0.007	0.000	0.001	
q_1^6	debye/Å^6	0.059	0.001	−0.116	−0.001	0.001	−0.001	0.003	
q_2q_3	debye/Å^2	0.427	0.002	0.112					
$q_2q_3^2$	debye/Å^3	0.077	−0.002						−0.001
$q_2^2q_3$	debye/Å^3	0.077	−0.002						−0.001

[a] The dipole moment function is expanded in the CH stretching coordinate as a Taylor series and the torsional coordinate in a Fourier series. The terms that are zero by symmetry have been left out. For the *x* and *z* components, the sin($m\theta$) diagonal and second order mixed stretching terms are zero. For the *y* component, the cos($m\theta$) diagonal and second order mixed stretching terms are zero.

Fourier series terms. We see that for *m*- and *p*-xylene the C_z component is well approximated by a constant plus cos(2θ) term, the C_x by a cos(θ) term and the C_y by a sin(θ) term as shown previously[8] and used in previous papers.[1,8,9,24] For *o*-xylene the angular dependence of the dipole expansion coefficients are still dominated by the terms in the above approximation however other terms become more important. As seen in Figure 4, the second-order diagonal coefficient is much closer to the constant plus cos(2θ) approximation than the first and fifth order coefficients.

The room-temperature vapor phase overtone spectra of *o*-, *m*-, and *p*-xylene in the CH stretching regions corresponding to $\Delta v_{CH} = 2-6$ are shown in Figures 5−9. The aryl regions of the spectra are described well by isolated local modes. In the higher overtone spectra the aryl peak separations increase and the isolated local modes become more obvious. In Figure 9, we see one aryl peak in the *p*-xylene spectra, two in *o*-xylene and three peaks for *m*-xylene, as expected. The complexity in the low-energy sides of the aryl $\Delta v_{CH} = 2$ region is due to local mode combination bands of the methyl group. The aryl region of the spectra in the $\Delta v_{CH} = 3-6$ regions, have been decomposed into a number of Lorentzian shape peaks corresponding to transitions for each of the nonequivalent CH bonds. The observed frequencies, absolute oscillator strengths ($\Delta v_{CH} = 2-3$), relative oscillator strengths ($\Delta v_{CH} = 2-6$), and assignment of these transitions are given in Tables 5, 6, and 7 as well as total intensities of the methyl regions.

The observed frequencies $\tilde{\nu}$ of the aryl local mode peaks have been fitted to a Birge−Sponer type expression[25]

$$\tilde{\nu}/v = \tilde{\omega} - (v+1)\tilde{\omega}x \qquad (6)$$

to obtain the local mode frequencies $\tilde{\omega}$ and anharmonicities $\tilde{\omega}x$ of the aryl CH oscillators. The parameters for *o*-, *m*-, and *p*-xylene are reported in Table 8.

The frequencies and anharmonicities of CH oscillators in the methyl group cannot be obtained in this fashion but are obtained from ab initio calculations. However, ab initio calculated frequencies and anharmonicities are often over estimated and scaling factors are applied.[38] We have calculated the local mode parameters of the aryl CH oscillator in *p*-xylene with the HF/6-31G(d) method. Comparison of the experimental and ab initio calculated local mode parameters lead to the scaling factors 0.9377 for the frequency and 0.907 for the anharmonicity. We have used these factors to scale the HF/6-31G(d) calculated local mode parameters of the methyl CH_1 oscillator in *o*-, *m*-, and *p*-xylene at the various torsional angles. These scaled local mode parameters were subsequently fitted to the Fourier series and the components of the fitted parameters are given in Table 1.

In our previous simulation of the methyl band profiles of toluene, we used scaled ab initio calculated local mode frequency and anharmonicity as a first approximation.[1] We improved these parameters by a best-fit procedure where we adjusted the parameters to obtain the best simulated spectra. The best fit is an improvement over the scaled ab initio parameters; however, for the xylenes we found that the simulation result with the scaled ab initio parameters agree well for most overtones and no best-fit procedure was performed.

The rotational constants *B* of the methyl groups of *o*-, *m*-, and *p*-xylene are calculated to be 5.46 cm^{-1}, 5.45 cm^{-1}, and 5.45 cm^{-1} respectively for the HF/6-31G(d) optimized geometries. The *B* values of the three molecules are very similar to

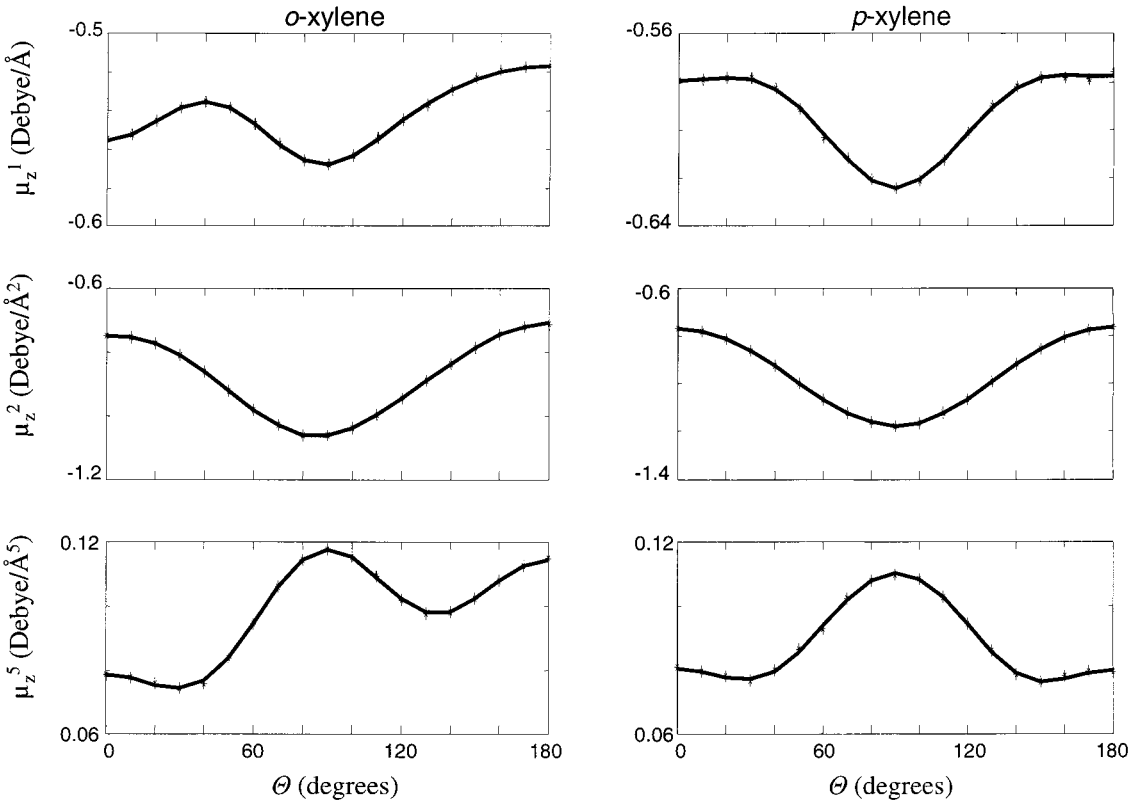

Figure 4. First, second and fifth order dipole moment displacement expansion coefficients are shown from top to bottom. We display the *z* component for *o*-xylene and *p*-xylene as a function of the torsional angle, θ. The asterisks represent the ab initio calculated results and the solid lines the Fourier series fit.

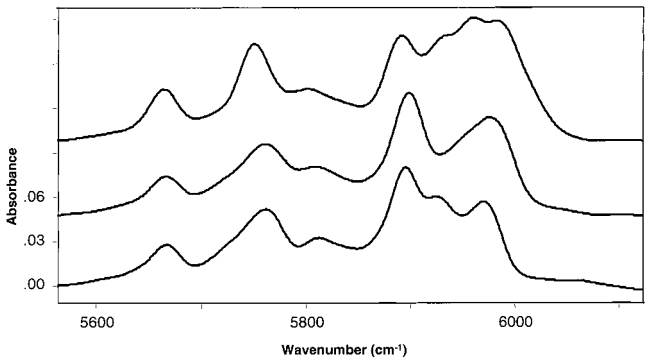

Figure 5. Room-temperature vapor phase overtone spectra of *o*-xylene (top), *m*-xylene (middle) and *p*-xylene (bottom) in the $\Delta v_{CH} = 2$ region. The spectra were measured with a path length of 4.75 m and pressures of 3 Torr for *o*-xylene and 4 Torr for *m*-xylene and *p*-xylene. The spectra of *o*- and *m*-xylene have been offset for clarity.

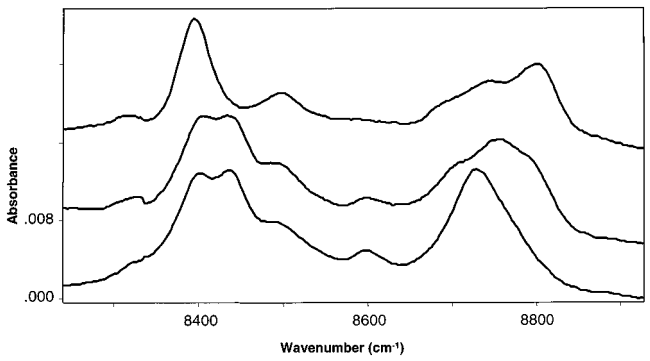

Figure 6. Room-temperature vapor phase overtone spectra of *o*-xylene (top), *m*-xylene (middle) and *p*-xylene (bottom) in the $\Delta v_{CH} = 3$ region. The spectra were measured with a path length of 4.75 m and pressures of 3 Torr for *o*-xylene and 4 Torr for *m*-xylene and *p*-xylene. The spectra of *o*- and *m*-xylene have been offset for clarity.

each other and to the value for toluene.[1] The *B* value decrease as the methyl CH oscillators are excited to higher CH stretching vibrational levels. It will differ slightly between the different vibrational states with the same total v and vary slightly with the torsional angle. However, we found these changes to have a minor effect on the simulated profiles and have not included them in our model. The effective coupling constant γ' of the methyl groups in *o*-, *m*-, and *p*-xylene have been calculated with the HF/6-31G(d) method to be 18.4 cm^{-1}, 18.8 cm^{-1}, and 18.5 cm^{-1}, respectively. Not surprisingly, the γ' values are similar to each other for the three molecules.

We have used the model outlined in the theory section with the parameters given in Tables 1−4 and 8 to calculate intensities of each of the aryl transitions and the total intensities of the simulated methyl band profiles. The results are listed in Tables 5−7 for *o*-, *m*-, and *p*-xylene.

We can analyze the aryl CH stretching transitions in relation to their positions with respect to the various CH_3 groups. In *p*-xylene the four aryl CH bonds are equivalent and only one peak is observed in the overtone spectra. All four CH oscillators are next to one electron donating CH_3 group and two positions away from the other CH_3 group. In *o*-xylene, the aryl CH oscillators at the 3 and 6 positions in the ring are in an identical environment, and the calculated CH bond lengths and local mode parameters are the same for each of these CH bonds as seen in Figure 1 and Table 8. The CH stretching intensities on a per CH bond basis for the aryls in *p*-xylene and 3,6 positions in *o*-xylene are also similar as seen in Tables 5 and 7. The CH oscillators in the 4 and 5 positions in *o*-xylene are further away from the electron donating CH_3 groups and the bond lengths are shorter, the CH stretching frequencies higher, and the transitions are more intense. In *m*-xylene there are three

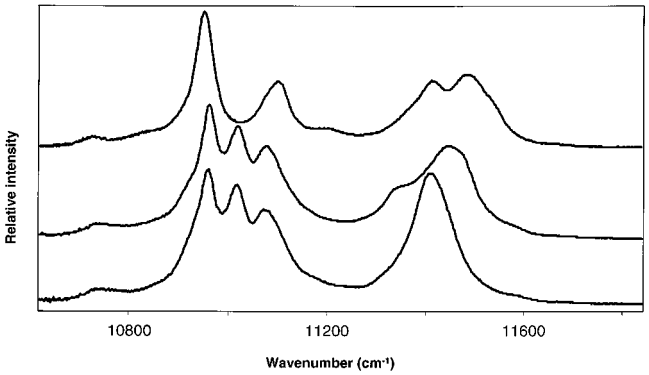

Figure 7. Room-temperature vapor phase overtone spectra of *o*-xylene (top), *m*-xylene (middle) and *p*-xylene (bottom) in the $\Delta v_{CH} = 4$ region. The spectra were measured by ICL-PAS with sample pressures of 3 Torr for *o*-xylene and 4 Torr for *m*-xylene and *p*-xylene. Argon buffer gas pressures of 182 Torr for *o*-xylene, 230 Torr for *m*-xylene and 230 Torr for *p*-xylene were used. The spectra of *o*- and *m*-xylene have been offset for clarity.

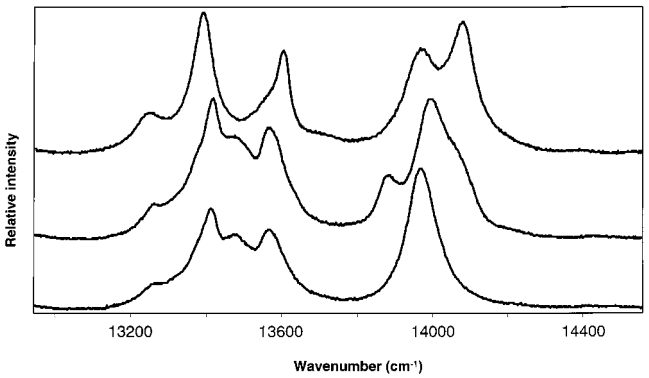

Figure 8. Room-temperature vapor phase overtone spectra of *o*-xylene (top), *m*-xylene (middle) and *p*-xylene (bottom) in the $\Delta v_{CH} = 5$ region. The spectra were measured by ICL-PAS with a sample pressure of 3 Torr for *o*-xylene and 4 Torr for *m*-xylene and *p*-xylene. Argon buffer gas pressures of 178 Torr for *o*-xylene, 120 Torr for *m*-xylene and 175 Torr for *p*-xylene were used. The spectra of *o*- and *m*-xylene have been offset for clarity.

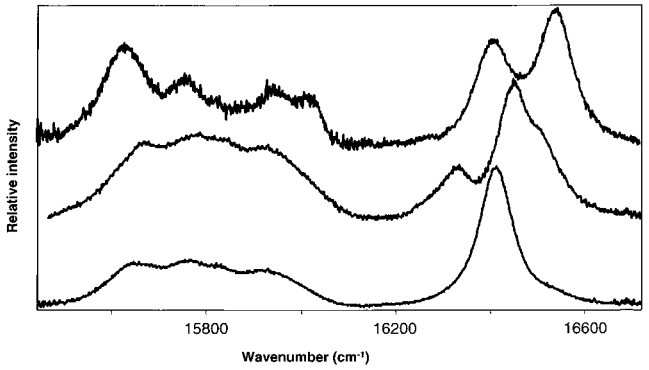

Figure 9. Room-temperature vapor phase overtone spectra of *o*-xylene (top), *m*-xylene (middle) and *p*-xylene (bottom) in the $\Delta v_{CH} = 6$ region. The spectra were measured by ICL-PAS with sample pressures of 3 Torr for *o*-xylene and 4 Torr for *m*-xylene and *p*-xylene. The lower energy methyl region was recorded with the dye DCM and argon buffer gas pressures of 200 Torr for *o*-xylene, 142 Torr for *m*-xylene and 131 Torr for *p*-xylene. The higher energy aryl regions of the spectra were recorded with the dye R6G and argon buffer gas pressures of 270 Torr for *o*-xylene, 250 Torr for *m*-xylene and 220 Torr for *p*-xylene. The spectra of *o*- and *m*-xylene have been offset for clarity.

nonequivalent aryl CH bonds. The CH bond in the 2 position has two neighboring CH_3 groups which both donate electron density making this bond the longest of the aryl CH bonds in all three xylene molecules and the one with the lowest CH stretching frequency as seen in Table 8. This CH bond in *m*-xylene is also the weakest transition on a per CH bond basis. In *m*-xylene, the CH bonds in the 4 and 6 positions are similar to the *p*-xylene aryl CH bonds but slightly shorter and slightly higher CH stretching frequency. The *m*-xylene aryl CH in the 5 position is furthest away from the CH_3 groups and have the shortest bond and highest CH stretching frequency. Thus, the effect of the electron donating CH_3 group on neighboring aryl CH bonds is to increase the CH bond length, lower the CH stretching frequency and reduce the intensity. The agreement

TABLE 5: Observed and Calculated Oscillator Strengths, Observed Frequencies and Peak Assignments for the CH Stretching Overtone Spectra of Vapor Phase *o*-Xylene

	observed			calculated[b]	
assignt[a]	$\tilde{\nu}$/cm^{-1}	absolute	relative[c]	absolute	relative[c]
$\|2\rangle$		5.3×10^{-7}		8.8×10^{-7}	
$\|3\rangle_m$		2.9×10^{-8}	0.48	9.6×10^{-8}	0.57
$\|3\rangle_{3,6}$	8735	2.0×10^{-8}	0.34	3.0×10^{-8}	0.18
$\|3\rangle_{4,5}$	8802	1.1×10^{-8}	0.18	4.0×10^{-8}	0.25
$\|3\rangle$		6.0×10^{-8}		1.7×10^{-7}	
$\|4\rangle_m$			0.55	1.1×10^{-8}	0.57
$\|4\rangle_{3,6}$	11406		0.22	3.7×10^{-9}	0.18
$\|4\rangle_{4,5}$	11497		0.24	5.0×10^{-9}	0.25
$\|4\rangle$				2.0×10^{-8}	
$\|5\rangle_m$			0.51	1.5×10^{-9}	0.57
$\|5\rangle_{3,6}$	13968		0.24	4.9×10^{-10}	0.18
$\|5\rangle_{4,5}$	14081		0.25	6.5×10^{-10}	0.24
$\|5\rangle$				2.7×10^{-9}	
$\|6\rangle_m$				2.4×10^{-10}	0.58
$\|6\rangle_{3,6}$	16406			7.5×10^{-11}	0.18
$\|6\rangle_{4,5}$	16542			9.8×10^{-11}	0.24
$\|6\rangle$				4.1×10^{-10}	

[a] Subscript m indicates total methyl bands. The numeric subscripts refer to the position on the ring of the aryl CH oscillators. The states $|v\rangle$ indicate total overtone intensities. [b] Calculated with the parameters in Tables 1 and 8 and the dipole moment function in Table 2. [c] The relative intensities are set to 1 for each vibrational overtone.

TABLE 6: Observed and Calculated Oscillator Strengths, Observed Frequencies and Peak Assignments for the CH Stretching Overtone Spectra of Vapor Phase *m*-xylene

	observed			calculated[b]	
assignt[a]	$\tilde{\nu}$/cm^{-1}	absolute	relative[c]	absolute	relative[c]
$\|2\rangle$		4.0×10^{-7}		8.8×10^{-7}	
$\|3\rangle_m$		2.1×10^{-8}	0.53	1.0×10^{-7}	0.62
$\|3\rangle_2$	8707	6.8×10^{-9}	0.17	1.2×10^{-8}	0.07
$\|3\rangle_{4,6}$	8757	8.5×10^{-9}	0.21	3.4×10^{-8}	0.20
$\|3\rangle_5$	8797	3.6×10^{-9}	0.09	1.9×10^{-8}	0.11
$\|3\rangle$		4.0×10^{-8}		1.7×10^{-7}	
$\|4\rangle_m$			0.59	1.2×10^{-8}	0.61
$\|4\rangle_2$	11346		0.08	1.5×10^{-9}	0.07
$\|4\rangle_{4,6}$	11438		0.28	4.2×10^{-9}	0.20
$\|4\rangle_5$	11477		0.06	2.4×10^{-9}	0.12
$\|4\rangle$				2.0×10^{-8}	
$\|5\rangle_m$			0.58	1.7×10^{-9}	0.60
$\|5\rangle_2$	13879		0.05	2.1×10^{-10}	0.08
$\|5\rangle_{4,6}$	13995		0.27	5.6×10^{-10}	0.20
$\|5\rangle_5$	14070		0.10	3.1×10^{-10}	0.11
$\|5\rangle$				2.7×10^{-9}	
$\|6\rangle_m$				2.6×10^{-10}	0.61
$\|6\rangle_2$	16321			3.4×10^{-11}	0.08
$\|6\rangle_{4,6}$	16445			8.6×10^{-11}	0.20
$\|6\rangle_5$	16510			4.8×10^{-11}	0.11
$\|6\rangle$				4.3×10^{-10}	

[a] Subscript *m* indicates total methyl bands. The numeric subscripts refer to the position on the ring of the aryl CH. The states $|v\rangle$ indicate total overtone intensities. [b] Calculated with the parameters in Tables 1 and 8 and the dipole moment function in Table 3. [c] The relative intensities are set to 1 for each vibrational overtone.

TABLE 7: Observed and Calculated Oscillator Strengths, Observed Frequencies, and Peak Assignments for the CH Stretching Overtone Spectra of Vapor Phase *p*-Xylene

	observed			calculated[b]	
assignt[a]	$\tilde{\nu}$/cm^{-1}	absolute	relative[c]	absolute	relative[c]
$\|2\rangle$		5.2×10^{-7}		9.0×10^{-7}	
$\|3\rangle_m$		4.3×10^{-8}	0.57	1.1×10^{-7}	0.64
$\|3\rangle_a$	8733	3.2×10^{-8}	0.43	6.2×10^{-8}	0.36
$\|3\rangle$		7.5×10^{-8}		1.7×10^{-7}	
$\|4\rangle_m$			0.59	1.3×10^{-8}	0.62
$\|4\rangle_a$	11412		0.41	7.6×10^{-9}	0.38
$\|4\rangle$				2.0×10^{-8}	
$\|5\rangle_m$			0.58	1.7×10^{-9}	0.63
$\|5\rangle_a$	13972		0.42	1.0×10^{-9}	0.37
$\|5\rangle$				2.7×10^{-9}	
$\|6\rangle_m$				2.6×10^{-10}	0.64
$\|6\rangle_a$	16411			1.5×10^{-10}	0.36
$\|6\rangle$				4.2×10^{-10}	

[a] Subscript m and a indicate total methyl and aryl bands. The states $|\upsilon\rangle$ indicate total overtone intensities. [b] Calculated with the parameters in Tables 1 and 8 and the dipole moment function in Table 4. [c] The relative intensities are set to 1 for each vibrational overtone.

between calculated and observed relative aryl intensities is generally good. However, the observed intensities for the $|3\rangle_{3,6}$ transitions in *o*-xylene and $|3\rangle_2$ transition in *m*-xylene are somewhat stronger than predicted by theory.[21] This discrepancy is likely to arise from couplings not included in our model.

On the basis of the number of hydrogen atoms we would expect the methyl to aryl oscillator strength ratios to be 6:4 which is close to what we observe for the regions $\Delta\upsilon_{CH} = 3-6$. The observed and calculated relative oscillator strengths of methyl and aryl transitions for each overtone are given in Tables 5−7. There is a good agreement between the observed and the calculated relative intensities as we also found for toluene.[1,8,9] In the highest overtone region, $\Delta\upsilon_{CH} = 6$, the spectra were measured with two laser dyes and spliced together which explains the slightly poorer agreement between observed and calculated relative intensities.

The observed and calculated absolute total CH stretching oscillator strengths are given in Tables 5−7. Absolute CH stretching overtone intensities calculated with a HF/6-31G(d) dipole moment function are expected to be significantly higher than the observed values and furthermore the discrepancy increases with υ.[39,40] This is in agreement with the results in Tables 5−7. In the $\Delta\upsilon_{CH} = 2$ region the observed oscillator strengths of *o*-, *m*-, and *p*- xylene are similar and about a factor of 3 less than the calculated values. In the $\Delta\upsilon_{CH} = 3$ region the calculations predict all three molecules to have similar intensities, whereas our measured values differ by almost a factor of 2 most likely due to significant uncertainty in the measure absolute intensities. The samples have relatively low vapor pressures that were not accurately measured.

We have previously shown that an HF/6-31G(d) calculated dipole moment function can predict well relative intensities of transitions to nonequivalent CH oscillators.[13,14,16] We thus assume that this limited ab initio method is adequate to model the stretching torsional coupling and to simulate the methyl spectral profiles. In Figures 10−12 we compared the observed and simulated spectral profiles of the $\Delta\upsilon_{CH} = 3-6$ methyl regions in *o*-, *m*-, and *p*-xylene. The observed methyl profiles of *m*- and *p*-xylene are similar and significantly different from that of *o*-xylene. Our simulations successfully reproduce these features. The fact that our model is successful for such different torsional potentials suggests that the approximation of the CH stretching methyl torsional coupling within our model is good.

The CH stretching overtone spectrum of *o*-xylene is similar to that of dimethyl ether.[14] In dimethyl ether, the barrier to methyl internal rotation has 3-fold symmetry with a relatively high torsional barrier of 909 cm^{-1}.[41] The spectrum of dimethyl

TABLE 8: Local Mode Frequency and Anharmonicity (in cm^{-1}) of the Aryl CH Stretching Modes in Vapor Phase *o*-, *m*-, and *p*-Xylene[a]

	o-xylene		*m*-xylene			*p*-xylene
CH position	3, 6	4, 5	2	4, 6	5	3, 4, 5, 6
$\bar{\omega}$	3147 ± 2	3169 ± 1	3142 ± 9	3157 ± 2	3170 ± 6	3146 ± 1
$\bar{\omega}x$	58.9 ± 0.3	58.9 ± 0.2	60.7 ± 1.6	59.5 ± 0.3	59.8 ± 1.0	58.6 ± 0.2

[a] From a fit of the local mode frequencies in $\Delta\upsilon_{CH} = 3-6$ regions. Uncertainties are one standard deviation.

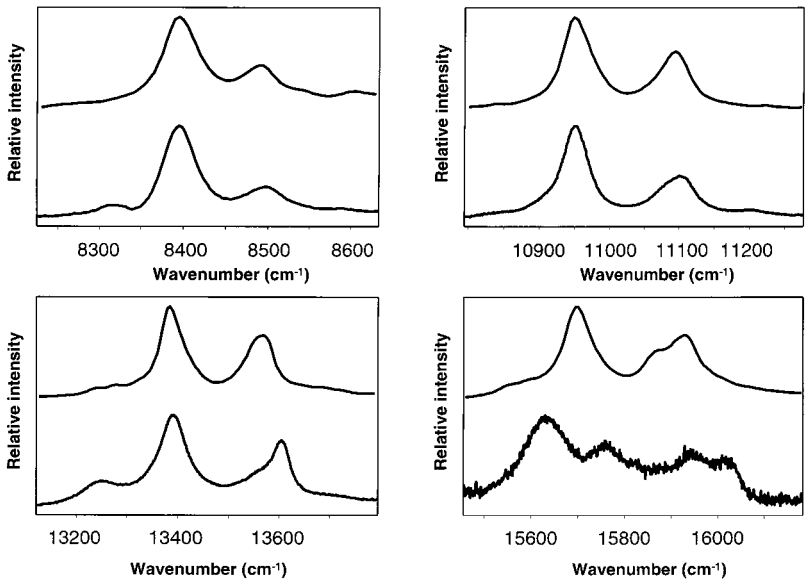

Figure 10. Observed (bottom) and simulated (top) spectra of *o*-xylene in the methyl regions of $\Delta\upsilon_{CH} = 3-6$.

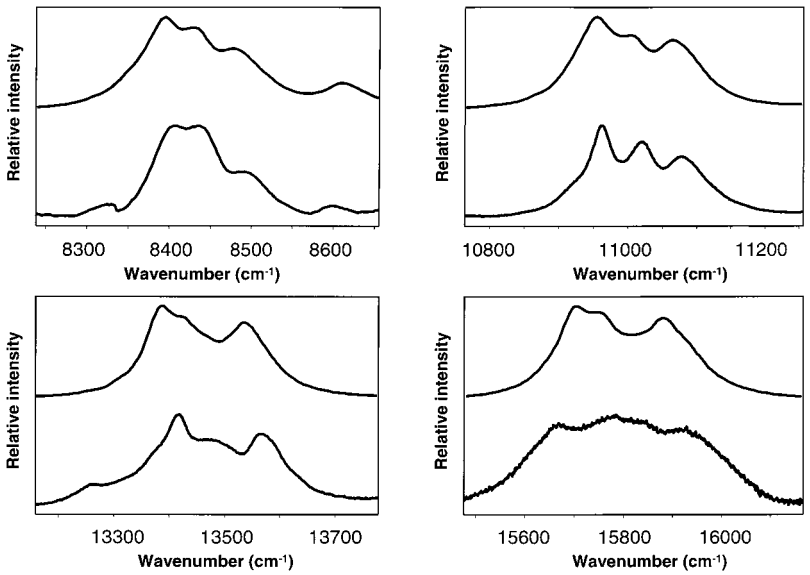

Figure 11. Observed (bottom) and simulated (top) spectra of *m*-xylene in the methyl regions of $\Delta v_{CH} = 3-6$.

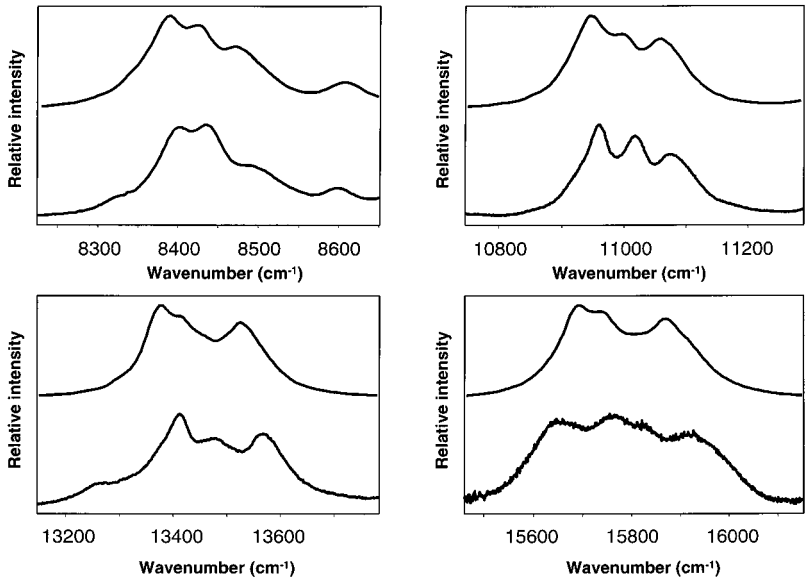

Figure 12. Observed (bottom) and simulated (top) spectra of *p*-xylene in the methyl regions of $\Delta v_{CH} = 3-6$.

ether is well described by a non rotating methyl group with two out-of-plane and one in-plane CH bonds.[14] The experimental barrier to internal rotation in *o*-xylene has a somewhat smaller V_3 barrier of 425 cm^{-1}.[12] However, the two-peak character of the methyl overtone spectrum of *o*-xylene seen in Figure 10 indicates that this barrier is still sufficiently high that the methyl group could be described as relatively fixed in one position with two out-of-plane CH bonds and one in-plane CH bond. The lower energy peak arises from the out-of-plane CH oscillators and the higher energy lower intensity peak arises from the in-plane CH oscillator. This assignment is in agreement with a calculated shorter in-plane CH bond length. The simulated spectra in Figure 10 are based on the treatment of the rotating methyl group as outlined in the theory section and not on a methyl group fixed in one position. The methyl band profiles shown in Figure 10 arise from a large number of transitions between vibrational-torsion states. The agreement between observed and simulated methyl band profiles is very good in the $\Delta v_{CH} = 3-5$ overtone regions. Thus, our generalized methyl rotor model seems to work well even when the torsional potential is high enough to warrant the use of the simpler model in which the methyl group fixed in one position.

The change from the "two peak" structure seen in dimethyl ether and *o*-xylene to the "three-peak" characteristic structure seen in the $\Delta v_{CH} = 4$ region of *m*- and *p*-xylene and in toluene, provides spectral evidence that torsional modes are actively coupled to the methyl CH stretching modes. The effect of this interaction increases as the barrier height decreases. If we compare to the overtone spectrum of acetone,[14] which has a torsional barrier of about 250 cm^{-1}, the intensity of the middle peak in the "three-peak" structure is smaller than in toluene, but larger than in *o*-xylene and perhaps the intensity of the center region is a measure of the barrier height.

Our simulated methyl profiles in the $\Delta v_{CH} = 6$ region are not as good as in the $\Delta v_{CH} = 3-5$ regions. The observed $\Delta v_{CH} = 6$ methyl band profiles of *o*-, *m*-, and *p*-xylene all seem to have more intensity in the center region than predicted by our simulations. This center region is also observed to be stronger than in the $\Delta v_{CH} = 5$ region. Furthermore the observed overall methyl bandwidths seem to be larger than in our simulated spectra at $\Delta v_{CH} = 6$. Both these features suggest the presence of additional coupling at the higher overtones, possibly due to Fermi resonance interactions between CH-stretching and HCH

bending modes or breakdown of the harmonic coupling approximation in the HCAO model.

Conclusion

We have used conventional and intracavity laser photoacoustic spectroscopy to record the vapor phase overtone spectra of *o*-, *m*-, and *p*-xylene in the regions of $\Delta v_{CH} = 2-6$. The absolute oscillator strengths for $\Delta v_{CH} = 2$ and 3 and relative oscillator strengths for $\Delta v_{CH} = 2-6$ have been measured.

The aryl regions of the *o*-, *m*-, and *p*-xylene spectra have been analyzed with a simple local mode model of isolated anharmonic oscillators. The methyl group is described with a model that includes coupling between the CH stretching and methyl torsional modes via both the Hamiltonian and the dipole moment function. The model describes the CH stretching modes within the HCAO local mode model and the methyl torsional modes in a rigid rotor basis. Variations of the torsional potential and the CH stretching frequency and anharmonicity with the torsional angle are included in the Hamiltonian. The dipole moment function is obtained from a series of ab initio calculations and includes dependence on the CH stretching displacement coordinates and for the methyl group also the torsional angle. Our model can accommodate arbitrary functional forms of the torsional potential, frequency and anharmonicity.

The relative intensities of the nonequivalent aryl CH oscillators and the relative aryl to methyl intensities are reproduced well by our calculations. The methyl band profiles in the *o*-, *m*-, and *p*-xylene spectra have been successfully simulated. These molecules encompass both a low energy 6-fold barrier and a relatively high energy 3-fold barrier to internal methyl rotation. The model accounts well for the change in methyl band profiles between these different types of torsional barrier.

Acknowledgment. We would like to thank Daryl L. Howard for help with the experiments. Z.R. is grateful to the University of Otago for a Specified Research Scholarship. H.G.K. is grateful to CIRES for a visiting faculty fellowship. The University of Otago and the Marsden Fund administrated by the Royal Society of New Zealand have provided funding for this research

References and Notes

(1) Kjaergaard, H. G.; Rong, Z.; McAlees, A. J.; Howard, D. L.; Henry, B. R. *J. Phys. Chem.* A **2000**, *104*, 6398.
(2) Hayward, R. J.; Henry, B. R. *J. Mol. Spectrosc.* **1975**, *57*, 221.
(3) Henry, B. R. *Acc. Chem. Res.* **1977**, *10*, 207.
(4) Mortensen, O. S.; Henry, B. R.; Mohammadi, M. A. *J. Chem. Phys.* **1981**, *75*, 4800.
(5) Child, M. S.; Lawton, R. T. *Faraday Discuss. Chem. Soc.* **1981**, *71*, 273.
(6) Sage, M. L.; Jortner, J. *Adv. Chem. Phys.* **1981**, *47*, 293.
(7) Child, M. S.; Halonen, L. *Adv. Chem. Phys.* **1984**, *57*, 1.
(8) Kjaergaard, H. G.; Turnbull, D. M.; Henry, B. R. *J. Phys. Chem. A* **1997**, *101*, 2589.
(9) Kjaergaard, H. G.; Turnbull, D. M.; Henry, B. R. *J. Phys. Chem. A* **1998**, *102*, 6095.
(10) Gough, K. M.; Henry, B. R. *J. Phys. Chem.* **1984**, *88*, 1298.
(11) Borst, D. R.; Pratt, D. W. *J. Chem. Phys.* **2000**, *113*, 3658.
(12) Breen, P. J.; Warren, J. A.; Bernstein, E. R.; Seeman, J. I. *J. Am. Chem. Soc.* **1987**, *109*, 3453.
(13) Kjaergaard, H. G.; Yu, H.; Schattka, B. R.; Henry, B. R.; Tarr, A. W. *J. Chem. Phys.* **1990**, *93*, 6239.
(14) Kjaergaard, H. G.; Henry, B. R.; Tarr, A. W. *J. Chem. Phys.* **1991**, *94*, 5844.
(15) Anastasakos, L.; Wildman T. A. *J. Chem. Phys*. **1993**, *99*, 9453.
(16) Kjaergaard, H. G.; Henry, B. R. *J. Chem. Phys.* **1992**, *96*, 4841.
(17) Cavagnat, D.; Lespade, L.; Lapouge, C. *J. Chem. Phys.* **1995**, *103*, 10 502.
(18) Cavagnat, D.; Lespade, L. *J. Chem. Phys.* **1998**, *108*, 9275.
(19) Cavagnat, D.; Lespade, L. *J. Chem. Phys.* **1997**, *106*, 7946.
(20) Cavagnat, D.; Lespade, L. *J. Chem. Phys.* **2001**, *114*, 6041.
(21) Cavagnat, D.; Lespade, L. *J. Chem. Phys.* **2001**, *114*, 6030.
(22) Cavagnat, D.; Lespade, L. *J. Chem. Phys.* **1998**, *102*, 8393.
(23) Bergeat, A.; Cavagnat, D.; Lapouge, C.; Lespade, L. *J. Phys. Chem. A* **2000**, *104*, 9233.
(24) Zhu, C.; Kjaergaard, H. G.; Henry, B. R. *J. Chem. Phys.* **1997**, *107*, 691.
(25) Atkins, P. W. *Molecular Quantum Mechanics*, 2nd ed.; Oxford University: Oxford, U.K., 1983.
(26) Henry, B. R.; Sowa, M. G. *Prog. Anal. Spectrosc.* **1989**, *12*, 349.
(27) Henry, B. R.; Kjaergaard, H. G.; Niefer, B.; Schattka, B. J.; Turnbull, D. M. *Can. J. Appl. Spectrosc.* **1993**, *38*, 42.
(28) Thomas, L. J., III.; Kelly, M. J.; Amer, N. M. *Appl. Phys. Lett.* **1978**, *32*, 736.
(29) Schattka, B. J.; Turnbull, D. M.; Kjaergaard, H. G.; Henry, B. R. *J. Phys. Chem.* **1995**, *99*, 6327.
(30) Kjaergaard, H. G.; Turnbull, D. M.; Henry, B. R. *J. Chem. Phys.* **1993**, *99*, 9438.
(31) MATLAB 6.0 release 12 from MathWorks Inc.
(32) Frisch, M. J.; Trucks, G. W.; Schlegel, H. B.; Gill, P. M. W.; Johnson, B. G.; Robb, M. A.; Cheeseman, J. R.; Keith, T.; Petersson, G. A.; Montgomery, J. A.; Raghavachari, K.; Al-Laham, M. A.; Zakrzewski, V. G.; Ortiz, J. V.; Foresman, J. B.; Cioslowski, J.; Stefanov, B. B.; Nanayakkara, A.; Challacombe, M.; Peng, C. Y.; Ayala, P. Y.; Chen, W.; Wong, M. W.; Andres, J. L.; Replogle, E. S.; Gomperts, R.; Martin, R. L.; Fox, D. J.; Binkley, J. S.; Defrees, D. J.; Baker, J.; Stewart, J. P.; Head-Gordon, M.; Gonzalex, C.; Pople, J. A. *Gaussian 94*, revision D.4; Gaussian, Inc.: Pittsburgh, PA, 1995.
(33) Low, G. R.; Kjaergaard, H. G. *J. Chem. Phys*. **1999**, *110*, 9104.
(34) Sowa, M. G.; Henry B. R.; Mizugai Y. *J. Phys. Chem.* **1991**, *95*, 7659.
(35) Rong, Z.; Kjaergaard, H. G., unpublished.
(36) Gough, K. M.; Henry, B. R.; Wildman, T. A. *Theochem*. **1985**, *25*, 71.
(37) Suzuki, T.; Ikegami, T.; Fujii M.; Iwato, S. *Theochem.* **1999**, *461−2*, 79.
(38) Scott, A. P.; Radom, L. *J. Phys. Chem*. **1996**, *100*, 16 502.
(39) Kjaergaard, H. G.; Henry, B. R. *Mol. Phys.* **1994**, *83*, 1099.
(40) Kjaergaard, H. G.; Daub, C. D.; Henry, B. R. *Mol. Phys.* **1997**, *90*, 201.
(41) Durig, J. R.; Li, Y. S.; Groner, P. *J. Mol. Spectrosc.* **1976**, *62*, 159.